

INVESTIGATION AND SIMULATION OF A SCOTCH YOKE MECHANISM

Sándor Apáti 

*PhD student, Institutional Department of Machine Tools,
3515 Miskolc-Egyetemváros, e-mail: sandor.apati@swisskrono.com*

György Hegedűs 

*associate professor, Institutional Department of Machine Tools
3515 Miskolc-Egyetemváros, e-mail: gyorgy.hegedus@uni-miskolc.hu*

Abstract

This paper studies the electromechanical model of a jigsaw mechanism. The jigsaw is powered by a battery, which drives a DC motor. The rotational motion is converted into linear motion through a Scotch Yoke mechanism. The electromechanical equations are based on energy approach using the Lagrange-equation. The Lagrange function contains the energies of the model, i.e., the kinetic co-energy of the kinematic chain and the magnetic co-energy of the inductance. As regard the non-conservative elements their virtual works are written. The formulated equations of the jigsaw model allow us to examine this force-energy relationship.

Keywords: *scotch yoke, mechanism, Scilab*

1. Introduction

In the machining and manufacturing processes hand tools are crucial. The jigsaw is a common portable power tool that may be used to efficiently separate soft material or cut straight or curved slots, which can cut steel, fiberglass, aluminum, and other materials in addition to wood, making them a highly useful tool in a workshop. Mehta and Patel studied a jigsaw machine's ability to cut several types of wood and metals of varying thicknesses is evaluated using kinematic and stress analysis. While designing, it is crucial to analyse the mechanism in relation to the rotation of the motor because the torque, active and constraint forces, and acceleration tend to change depending on the angular position of the rotating spindle, which in turn alters the inertia forces and stresses in the mechanism. The results of this study show the maximum von Mises stress values and the maximum input power demand, which are compared with the material qualities and the specifications of the jigsaw machine, respectively, and the performance of the machine has been assessed (Mehta et al., 2017).

Research was conducted to examine material removal in reciprocating sawing as part of an attempt to model cutting and enhance blade design. Results from an experimental cutting fixture demonstrated that linear cutting rates rise with both reciprocating rate and thrust force, while the evidence suggests that thrust force may be more useful for cutting optimization. Additionally, it was discovered that using a blade cannot create an angled cut and causes a dynamic thrust force that alternately works against and for the user. According to research, most of the material removal occurs during the cutting stroke, when around two thirds of the chips are produced (Domblesky et al., 2006).

The reciprocating sawing process was examined by (Domblesky et al., 2008) along with a model for linear cutting rate. The final model takes into consideration elastic and plastic indentation and is based on an orthogonal approximation of cutting at individual teeth. For the variety of variables taken into consideration, cutting rates achieved from an instrumented sawing fixture demonstrate good agreement with projected results. Cutting rate was discovered to be inversely related to thrust force and reciprocating rate, albeit at higher levels, edge radius and flow stress have an impact on this behavior. The influence of pitch and blade configuration could not be separated; however, it was established that blades with a coarser pitch do indeed cut more quickly (Domblesky et al., 2008).

When examining jigsaws, it is important to determine the direction of sawing. In the case of the type of saw to be tested, the machine has a so-called blade tilting unit, which allows the saw blade to only cut in one direction. After determining the cutting direction, it is important to define the cut material, wood is assumed generally. The basic requirement of a good saw, according to which the blade made of steel is of high quality. Saw blades made of electro- or cast steel alloyed with chrome and vanadium, whose toughness and flexibility, as well as their ability to hold an edge, are both favorable. Furthermore, with these saw blades, high performance can be produced with low energy input.

The demand for vibration reduction in handheld tools is important in order to provide this requirement a damper design is taken into consideration. The examination of vibration exposure and damper may be determined with the use of jigsaw power tool analysis. The primary goal of this work is to evaluate the exposures to vibrations created in the hand or body when using power tools. The utilization of dampening devices to reduce vibration in handheld power machines is summarized in this work. By strategically placing a damper on a power tool, the vibration emission may be detected and regulated. This design guide's goal is to assist the design engineer in making the right damping device selection to lessen the amount of vibration or noise (Koli et al., 2015), (Patil et al., 2016).

The purpose of the experimental and theoretical investigation of the battery-powered jigsaw is primarily to determine how the cutting force affects the battery charge. What are the parameters that may be changed to achieve more cutting cycles at a specific battery charge level. In addition to the parameters of the battery, it is necessary to know the physical characteristics of the mechanical parts connected to the engine of the saw, e.g., moments of inertia. It is advisable to describe the production of the mathematical model using the energy method (Yifei, 2018), (Manhães et al., 2018), because in this way the electrical and mechanical systems can be handled uniformly. For this, the additional kinetic energy of the entire kinematic chain and the additional magnetic energy stored in the coil of the electric motor must be determined. In relation to the non-conservative elements (resistance, voltage source, friction, etc.), it is necessary to describe the increment of the virtual work (Preumont, 2006). In possession of these quantities, a system of coupled differential equations can be produced by applying the Lagrange equation of the 2nd kind. The equations provide parameter studies with numerical simulation, which show the dynamic and electrical behavior of the model.

Scotch yoke is one of the known mechanisms used for converting rotational motion into reciprocating motion or vice versa. In this motion transforming device, the reciprocating part like a piston is rigidly connected to yoke link featuring a slot which is engaged with a pin fitted to rotating part. For constant rotational speed, the mechanism allows sinusoidal reciprocating motion with constant amplitude and frequency. The kinematic and dynamic properties of these mechanisms are well studied (Al-Hamood et al., 2019), (Sawyer et al., 2003).

2. Mechanical Model of Scotch Yoke Mechanism

The electromechanical model of the jigsaw is schematically illustrated in *Figure 1*. Regarding the DC motor, the voltage source U_0 and internal resistance R_b of the battery are given, as well as the resistance and inductance L of the coil. Based on (Preumont, 2006), the voltage U_i induced by the motor rotor is determined by the speed and torque constant of the motor $k_e = k_m$. The J_m inertia of the rotor and the rotating and alternating masses of the entire kinematic chain connected to it provide the moment of inertia J_{red} of the system as a function of the angular rotation of the motor. The effective work of the saw is done by the cutting force F_v .

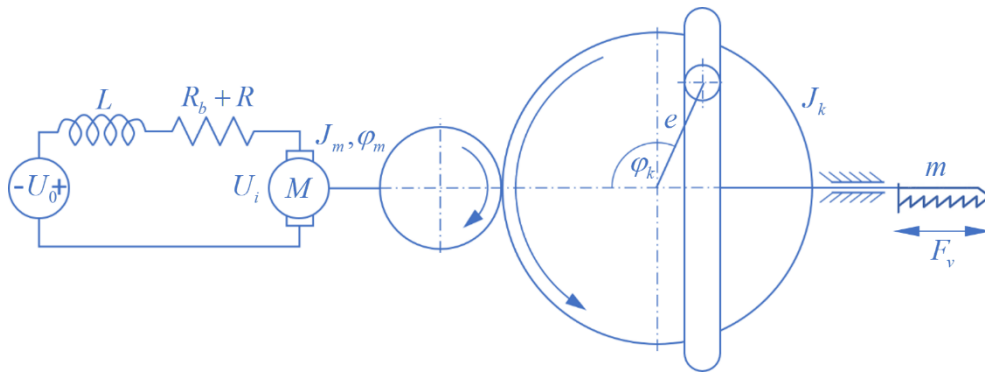


Figure 1. Model of coupled electromechanical system

For the electric motor, for a pulley gear, where J_m denotes the moment of inertia of the motor, the J_k is the moment of inertia of the gear unit, φ_k is the angular rotation m the mass of the blade the position of the pin and the F_v cutting force. Based on the created model, the Lagrange function can be written as:

$$\mathcal{L} = T^* + W_m^* = \frac{1}{2} J_r(\varphi_m) \dot{\varphi}_m^2 + \frac{1}{2} L \dot{q}^2 \quad (1)$$

where:

$$T^* = \frac{1}{2} J_m \dot{\varphi}_m^2 + \frac{1}{2} J_k \dot{\varphi}_k^2 + \frac{1}{2} m \dot{x}^2 = \frac{1}{2} \underbrace{\left[J_m + J_k k_{m,k}^2 + m e^2 k_{m,k}^2 \sin^2(k_{m,k} \varphi_m) \right]}_{J_r(\varphi_m)} \dot{\varphi}_m^2 \quad (2)$$

and

$$\begin{aligned}
 k_{m,k} &= \frac{z_m}{z_k}, \\
 \varphi_k &= k_{m,k} \varphi_m, \\
 \dot{\varphi}_k &= k_{m,k} \dot{\varphi}_m, \\
 \dot{x} &= \frac{dx}{d\varphi_m} \frac{d\varphi_m}{dt}.
 \end{aligned} \tag{3}$$

Where q is the charge, \dot{q} is the current, $k_{m,k}$ is gear ratio number z_k is determined by the number of teeth of the motor and the driven gear z_m . The virtual work of non-conservative elements:

$$\delta W_{nc} = U_0 \delta q - (R + R_b) \dot{q} \delta q - k_e \dot{\varphi}_m \delta q + k_m \dot{q} \delta \varphi_m - \left[F_v e k_{m,k} \sin(k_{m,k} \varphi_m) \right] \delta \varphi_m - b \dot{\varphi}_m \delta \varphi_m \tag{4}$$

With the equations (1)–(4) based on the electrical equation of the system is generated using the second-order Lagrange equation:

$$\frac{d}{dt} \left(\frac{\partial L}{\partial \dot{q}} \right) - \frac{\partial L}{\partial q} = U_0 - (R + R_b) \dot{q} - k_e \dot{\varphi}_m, \tag{5}$$

$$\frac{d}{dt} \left(\frac{\partial L}{\partial \dot{q}} \right) = L\ddot{q}, \tag{6}$$

$$L\ddot{q} = U_0 - (R + R_b) \dot{q} - k_e \dot{\varphi}_m, \tag{7}$$

$$U_0 = L\ddot{q} + (R + R_b) \dot{q} + k_e \dot{\varphi}_m, \tag{8}$$

and the dynamic equation of motion can be written as

$$\frac{d}{dt} \left(\frac{\partial L}{\partial \dot{\varphi}_m} \right) - \frac{\partial L}{\partial \varphi_m} = k_m \dot{q} - \left[F_v e k_{m,k} \sin(k_{m,k} \varphi_m) \right] - b \dot{\varphi}_m, \tag{9}$$

$$\frac{\partial L}{\partial \dot{\varphi}_m} = J_r(\varphi_m) \dot{\varphi}_m, \tag{10}$$

$$\frac{d}{dt} (J_r(\varphi_m) \dot{\varphi}_m) = J_r(\varphi_m) \ddot{\varphi}_m + \frac{dJ_r(\varphi_m)}{d\varphi_m} \frac{d\varphi_m}{dt} \dot{\varphi}_m = J_r(\varphi_m)' \dot{\varphi}_m + J_r(\varphi_m) \dot{\varphi}_m^2, \tag{11}$$

$$\frac{\partial L}{\partial \varphi_m} = \frac{1}{2} J_{red}(\varphi_m)' \dot{\varphi}_m^2 \tag{12}$$

$$J_r(\varphi_m)\ddot{\varphi}_m + \frac{1}{2}J_r'(\varphi_m)\dot{\varphi}_m^2 = k_m\dot{q} - [F_v e k_{m,k} \sin(k_{m,k}\varphi_m)] - b\dot{\varphi}_m. \quad (13)$$

The coupled non-linear equation of system formulated by equation (8) and (13) provides the mathematical model of the simulation program.

3. Scilab Script and Simulation Results

Based on the mathematical model derived in the previously described chapter, an algorithm was developed in *Scilab* system which can be seen on *Figure 2*. The main parameters such as motor speed, current consumption and alternating movement of the blade are generated as a function of time.

Figure 2 shows the function *ScotchYoke* with global variables and required *ydot* output results vector. The *y* input variable is calculated by the built in *Scilab ode* ordinary differential equation solver, where the adaptive Runge–Kutta of order 4 (RK4) method was applied.

```

0001 function [ydot]=ScotchYoke(t, y)
0002     global Jm Jk kmk e m Fv L R ke km U0 b Rb
0003
0004     i_A= y(1)
0005     fim= y(2)
0006     dfim= y(3)
0007
0008     Jred= Jm + Jk*kmk^2 + (kmk*e)^2 * m * (sin(kmk*fim))^2
0009     dJ= kmk^3*e^2 * m * sin(2*kmk*fim)
0010
0011     Mv=0
0012     if sin(kmk*fim)>0 then
0013         Mv= Fv * kmk * e * sin(kmk*fim)
0014     end
0015
0016     Mm=km*i_A
0017
0018     ydot(1)= ( - (R+Rb)*i_A - ke * dfim + U0 ) / L
0019     ydot(2)= y(3)
0020     ydot(3)= ( -b * dfim -0.5 * dJ * dfim^2 + Mm - Mv )/Jred
0021 endfunction

0026 y=ode("rk",y0,t0,t,ScotchYoke);

```

Figure 2. Scilab script for calculation

Figure 3 illustrates the change in the revolution of the DC motor in the time interval 0–1 s. The motor picks up the operating speed very short time in 0.05 s, which typical property of the sawing mechanism, shows a rising character in time when it is not sawing and suddenly decreases its value under the load of sawing.

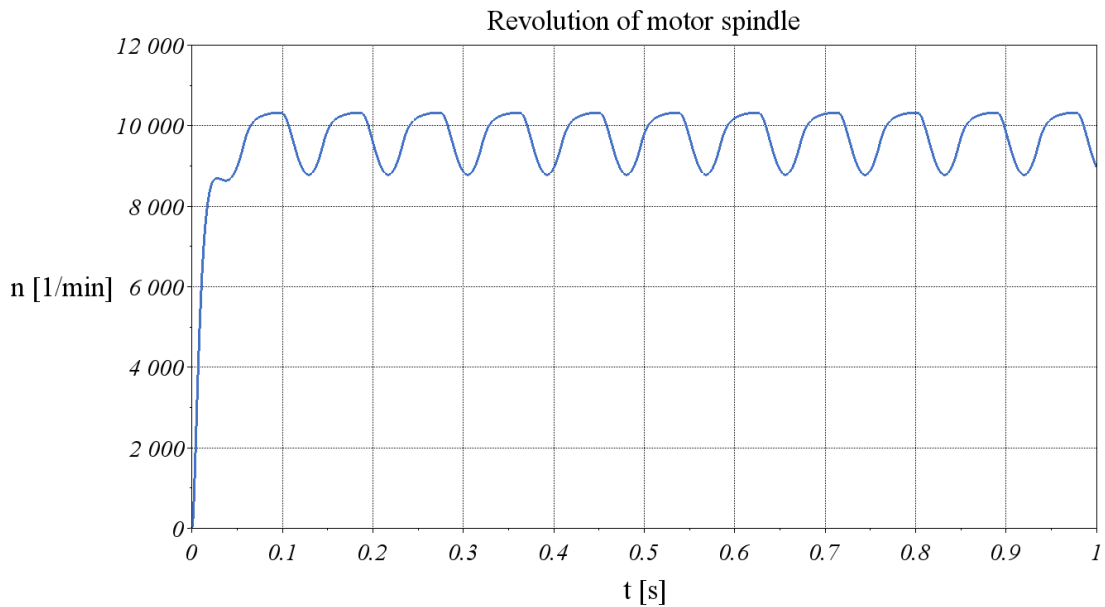


Figure 3. Revolution of motor spindle, $F_v = 200\text{ N}$

The current consumption of the DC motor is illustrated in Figure 4, where it can be seen that when the system is started, a short-circuit current (approximately 29A) occurs for a very short time, and then local peaks of approximately 7 A are formed due to the cutting force of the sawing. When the saw blade moves in unloaded condition, the current consumption drops to approximately 1 A.

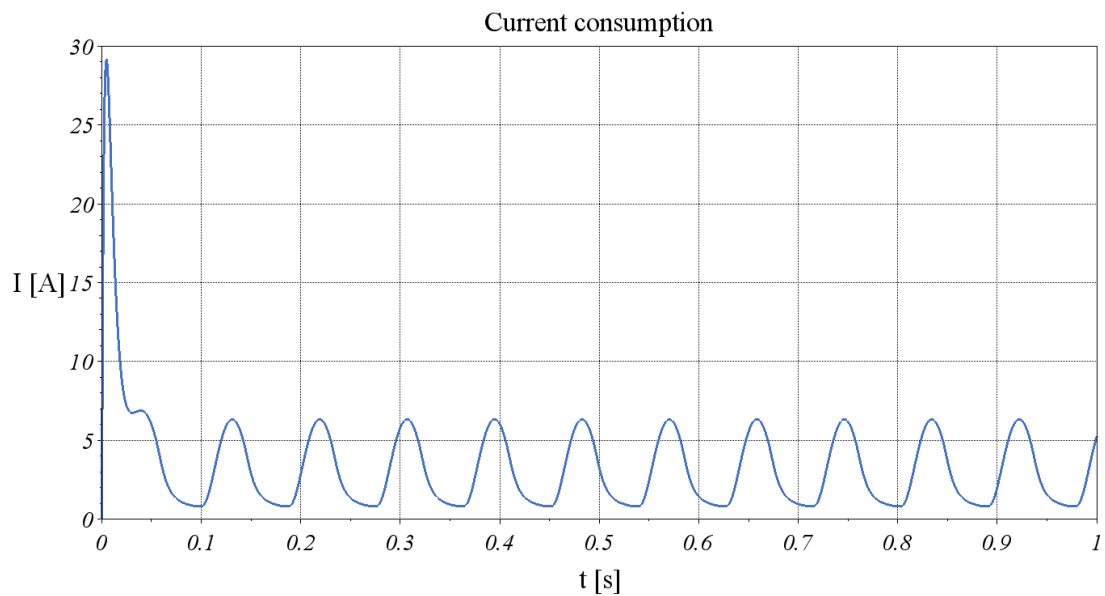


Figure 4. Current consumption of the system, $F_v = 200\text{ N}$

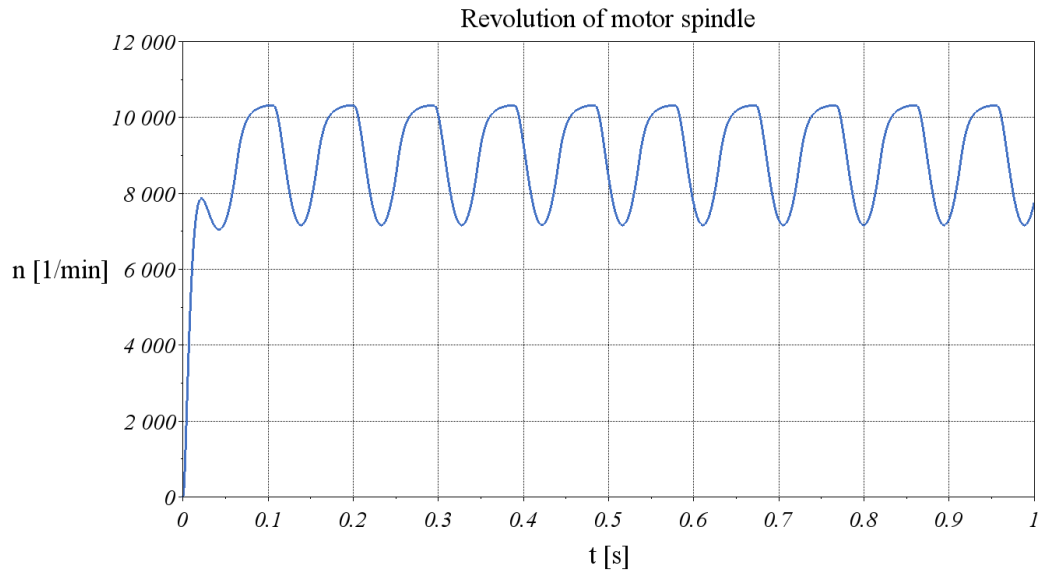


Figure 5. Revolution of motor spindle, $F_v = 400\text{ N}$

The previous figure clearly shows that the engine speed suddenly reaches the operating speed, which is near 0.1 s. By comparing Figure 3 with Figure 5, it can be seen that the peak value of the spindle revolution is not affected by the cutting force, however the local minimum values in the spindle revolution are lower on cutting force $F_v = 400\text{ N}$ compared with $F_v = 200\text{ N}$. This speed range is realized between $8,500\text{ min}^{-1}$ and $10,500\text{ min}^{-1}$. The reduction in cutting force clearly shows that this range is smaller than the motor speed range previously taken with doubled the sawing load. Figure 6 shows the current consumption under a load of $F_v = 400\text{ N}$.

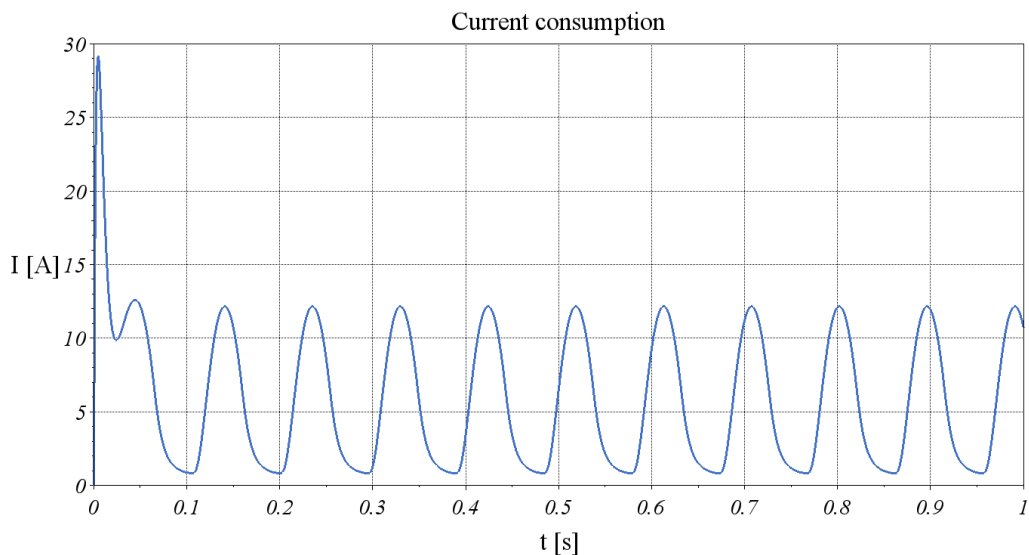


Figure 6. Current consumption of the system, $F_v = 400\text{ N}$

In this case, since the load is doubled as shown in the previous *Figure 4*, it can be seen that local peaks (approximately 13 A) are formed here, which shows that the motor of the jigsaw in this case needs near twice as much current as the previously measured under a load of $F_v = 200\text{ N}$.

4. Summary

A highly non-linear system of differential equations was created for the model of the jigsaw using the Lagrange equation. The electromechanical coupling is an essential tool to formulate a Lagrangian. To introduce the electromechanical coupling, it was necessary to present the difference between energy and coenergy and how energy is transferred from one place to another in an electromechanical model. Based on the coupled differential equations, a simulation program was developed under the *Scilab* system. The program can determine the speed of the motor, the current consumption, and the movement of the saw blade as a function of time. Calculations performed on different loads confirm the effective applicability of the developed model for further parameter tests.

Future plans include the development of a measuring and testing facility that investigates the electromechanical behavior of the jigsaw under various cutting conditions (i.e., bulk material, tool geometries, feed, rotational and oscillating speeds). Knowing the measured results, the electromechanical model can be refined, thus the reliability of further simulation runs can be improved.

References

- [1] Mehta, V., Patel, V. (2017). Performance Evaluation of Jigsaw Machine with Kinematic and Stress Analysis. *Proceedings of ICTACEM 2017 International Conference on Theoretical, Applied, Computational and Experimental Mechanics*, ICTACEM-2017/0655.
- [2] Domblesky, J., Widera, G. E. O., James, T. P. (2006). Experimental investigation of reciprocating sawing. *Transactions of the North American Manufacturing Research Institute of SME*, Vol. 34, pp. 531–538.
- [3] Domblesky, J. P., James, T. L., Widera, G. E. O. (2008). A Cutting Rate Model for Reciprocating Sawing. *Journal of Manufacturing Science and Engineering*, Vol. 130, No. 5. <https://doi.org/10.1115/1.2976143>
- [4] Koli, A. A., Tayde, M. M. (2015). Design and Analysis of Jigsaw and Damper for Effect of Vibration Reduction in Hand Held Power Tool. *International Journal of Emerging Technology and Advanced Engineering*, Vol. 5, No. 7, pp. 65–73.
- [5] Patil, N. B., Salunke, J. J. (2016). Design and Analysis of Viscous Damper for Vibration Reduction in Hand Operated Power Tools. *International Journal of Engineering Sciences & Research Technology*, Vol. 5, No. 2, pp. 514–524.
- [6] Yifei, H. (2019). The Motion Characteristics and Control Circuit of a Reciprocating Electric Jig Saw. *IEEE Xplore*, Nov. pp. 5314–5317, <https://doi.org/10.1109/CAC48633.2019.8996285>
- [7] Manhães, W., Sampaio, R., Lima, R., Hagedorn, P., Deü, J.-F. (2018). Lagrangians for Electromechanical Systems. *Mecánica Computacional*, Vol. 36, No. 42, pp. 1911–1934.

- [8] Preumont, A. (2006). *Mechatronics – Dynamics of Electromechanical and Piezoelectric Systems*. Springer. <https://doi.org/10.1007/1-4020-4696-0>
- [9] Al-Hamood, A., Jamali, H. U., Abdullah, O. I., Senatore, A. (2019). Dynamics and lubrication analyses of scotch yoke mechanism. *International Journal on Interactive Design and Manufacturing (IJIDeM)*, Vol. 13, No. 3, pp. 901–907, <https://doi.org/10.1007/s12008-019-00545-y>
- [10] Sawyer, W. G., Diaz, K. I., Hamilton, M., Micklos, A. B. (2003). Evaluation of a Model for the Evolution of Wear in a Scotch-Yoke Mechanism. *Journal of Tribology*, Vol. 125, No. 3, pp. 678–681, <https://doi.org/10.1115/1.1537271>
- [11] Vande Wouwer, A., Saucez, P., Vilas, C. M. (2014). *Simulation of ODE/PDE Models with MATLAB®, OCTAVE and SCILAB*, Springer Cham. ISBN 978-3-319-06790-2. <https://doi.org/10.1007/978-3-319-06790-2>
- [12] Roux, P. (2016). *Scilab from Theory to Practice - I. Fundamentals*, Editions D-Booker. ISBN 978-2822702935